All-DNA finite-state automata with finite memory

Zhen-Gang Wang[a,1], Johann Elbaz[a,1], F. Remacle[b], R. D. Levine[a,c,2], and Itamar Willner[a,2]

[a]Institute of Chemistry, Hebrew University of Jerusalem, Jerusalem 91904, Israel; [b]Chemistry Department, B6c, University of Liège, 4000 Liège, Belgium; and [c]Department of Chemistry and Biochemistry, Crump Institute for Molecular Imaging, and Department of Molecular and Medical Pharmacology, University of California, Los Angeles, CA 90095

Contributed by Raphael D. Levine, October 25, 2010 (sent for review August 6, 2010)

Biomolecular logic devices can be applied for sensing and nanomedicine. We built three DNA tweezers that are activated by the inputs H^+/OH^-; Hg^{2+}/cysteine; nucleic acid linker/complementary antilinker to yield a 16-states finite-state automaton. The outputs of the automata are the configuration of the respective tweezers (opened or closed) determined by observing fluorescence from a fluorophore/quencher pair at the end of the arms of the tweezers. The system exhibits a memory because each current state and output depend not only on the source configuration but also on past states and inputs.

biocomputing | DNA machines | sensor | chemical recognition | chemical input

Supramolecular systems that can be instructed by external triggers and interact with biological systems attract growing interest. Such combined assemblies hold the promise for future nano-medical and bioengineering applications (1–3). In particular, the base sequence in DNA enables recognition and self-assembly. We use these properties to operate a molecular assembly of "tweezers" that can be opened or closed by external inputs. The machine processes the inputs depending on its internal state and delivers an output. Such a machine is defined as an automaton. Indeed, the structural and functional information encoded in biomolecules such as DNA (4), DNAzymes (5, 6), ribozymes (7), DNA/protein hybrids (8), and enzymes (9) has been implemented to develop logic gates (10) and finite automata (11). The use of these logic devices to control gene expression (12), and to process intracellular information (13), was demonstrated. Also, programmed nucleic acid structures were used to design DNA machines (14–17), and supramolecular DNA nanostructures performing "walker," (18–22), "tweezers" (23–26), and "gear" (27) functionalities were reported, using nucleic acid strands, aptamer–substrate complexes (28), or pH (29, 30) as triggers (inputs) for the activation of DNA machinery devices. Previous studies described DNA–protein automata, and the advantages of an all-DNA automata device were theoretically addressed (31). The present study presents unique enzyme-free DNA automata, based on the use of new chemical inputs (Hg^{2+}/cysteine and H^+/OH^-) that require detailed design of the recognizing nucleic acids. There are eight possible configurations of the three tweezers (open/closed for each). A configuration is deemed an output of the system and is determined by reading out the fluorescence signals of the tweezers. These configurations change when inputs are provided; however, the next configuration will depend not only on the most recent input but on the past input history. Therefore we introduce the notion of "state" that, combined with the input, will uniquely determine the output and the next state. The states are hidden, but they can be unambiguously assigned at each step; as shown below, 16 states suffice to fully describe history-dependent response of the system. Such response is found in complex systems. For example, acquired magnetization of a ferromagnetic material reflects its past physical treatment.

Results and Discussion

Fig. 1*A* presents the elements of the device. It consists of three tweezers, α, β, γ, and six inputs (pH-acidic or basic; Hg^{2+} ions or cysteine ligands complexing Hg^{2+} ions; and two complementary single stranded nucleic acids acting as linker/antilinker units). Each of the tweezers may exist in the closed configuration "0" or the open structure configuration "1." Thus, the three tweezers may generate eight different configurations (outputs); two configurations where all three tweezers are closed (000) or open (111), respectively, three configurations consisting of one open tweezers and two closed, and three configurations that include two open tweezers and one closed. The general principles of the input-triggered opening or closing of the tweezers and the readout of the tweezers configuration are depicted in Fig. 1*B*. The tweezers consist of two nucleic acid arms (I and II) bridged by a "reporter" nucleic acid III that includes at its ends a fluorophore/quencher pair. The arms I and II are further bridged by complementary base pairing with the nucleic acid linker IV to form the closed tweezers. The domains Ia and IIb in the arms I and II provide the recognition sites for the respective inputs. While the inputs of type I_1 open the tweezers and release the linker, the addressing of the open tweezers with inputs of type I_2 results in the association of the linker to the arms and in the closure of the tweezers. The fluorescence resonance energy transfer (FRET) between the fluorophore and quencher transduces the configuration of the tweezers. While the proximity of the fluorophore/quencher pair in the closed tweezers leads to effective quenching and low fluorescence of the fluorophore, in the open configuration the fluorophore and quencher are apart, leading to a less efficient quenching, and a high fluorescence signal. By the labeling of each of the tweezers with a specific fluorophore [ROX(F_1), Cy5.5(F_2), Cy5(F_3)], the configuration of the respective tweezers (open or closed) is optically read out by the respective fluorescence labels. The domains Ia and IIb in the tweezers constructs are instructed to switch between the closed and open configurations by the respective inputs. The switching of tweezers α is exemplified in Fig. 2*A*. In their closed configuration the tweezers include the arms Ia and IIb bridged to the linker unit by Hg^{2+} ions through T-Hg^{2+}-T bonds

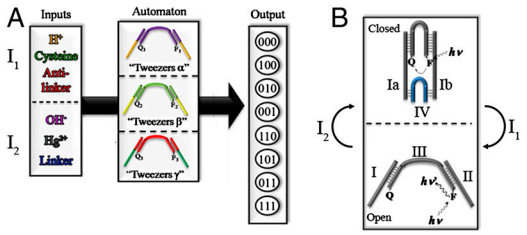

Fig. 1. (*A*) General scheme for the application of three-tweezers structures and a set of counteracting inputs (I_1 and I_2) to yield eight different configurations (outputs) in a finite-state automaton. (*B*) General scheme for the construction of the tweezers structure and its reversible opening/closure by the counter inputs I_1 and I_2, respectively.

Author contributions: Z.-G.W., J.E., and I.W. designed research; Z.-G.W., J.E., F.R., R.D.L., and I.W. performed research; and Z.-G.W., J.E., F.R., R.D.L., and I.W. wrote the paper.

The authors declare no conflict of interest.

[1]Z.-G.W. and J.E. contributed equally to this work.

[2]To whom correspondence may be addressed. E-mail: willnea@vms.huji.ac.il or rafi@fh.huji.ac.il.

This article contains supporting information online at www.pnas.org/lookup/suppl/doi:10.1073/pnas.1015858107/-/DCSupplemental.

www.pnas.org/cgi/doi/10.1073/pnas.1015858107

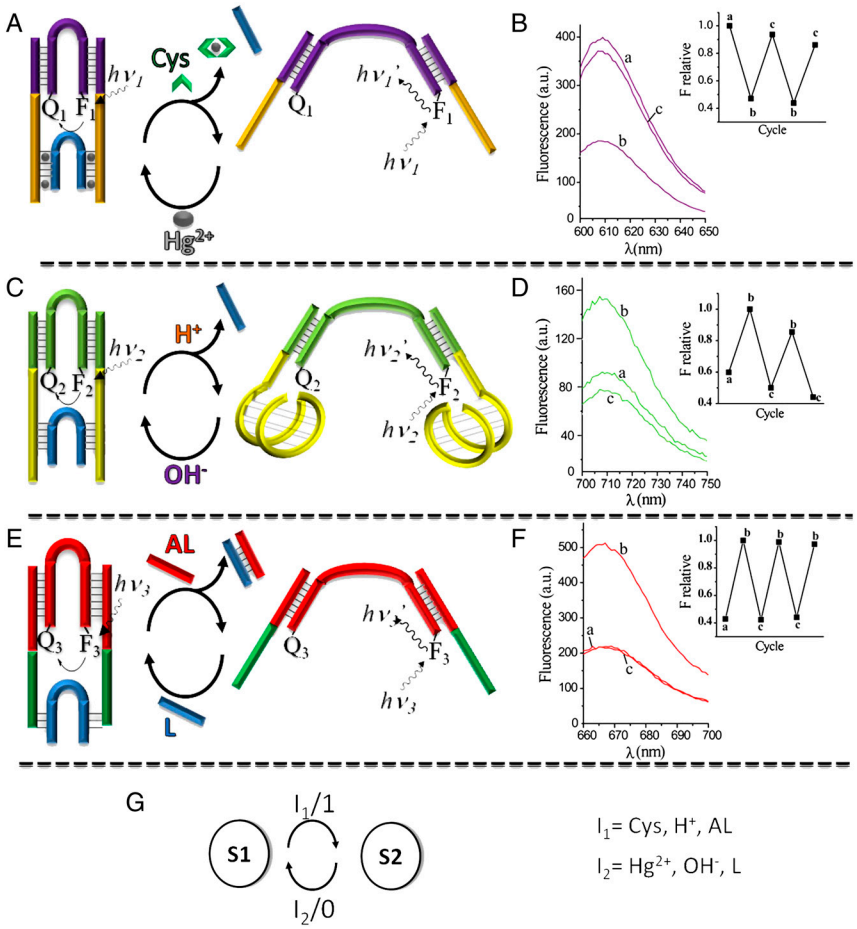

Fig. 2. (*A*) Schematic presentation of the concurrent activation of tweezers α using Hg^{2+} and cysteine as inputs that form the configurations "0" (closed) and "1" (opened), respectively. (*B*) Fluorescence spectra corresponding to the respective configuration of tweezers α: (a) Initial configuration of the tweezers, (1), with no added input. (b) After the addition of Hg^{2+} as input. (c) After the addition of the cysteine input. Inset: Cyclic activation of the tweezers between configurations (0, closed) (b) and (1, open) (c). (*C*) Schematic presentation of the opening and closing of tweezers β using H^+ and OH^-, as inputs that form the configurations (1) and (0), respectively. (*D*) Fluorescence spectra corresponding to the respective configurations of tweezers β : (a) Initial state of the tweezers, (0), with no added input at pH = 7.2. (b) After the addition of H^+ as input that changes the pH value to 5.2. (c) After the addition of the OH^- input. Inset: Cyclic activation of the tweezers between configurations (1) (b) and (0) (c). (*E*) Schematic presentation of the concurrent activation of tweezers γ using the linker (L) and antilinker (AL) as inputs that form the configurations (0) and (1), respectively. (*F*) Fluorescence spectra corresponding to the respective configurations of tweezers γ : (a) Initial configurations of the tweezers, (0), in the presence of the linker input. (b) After the addition of the antilinker as input. (c) After the addition of the linker input. Inset: Cyclic activation of the tweezers between configurations (1) (b) and (0) (c). (*G*) Schematic presentation of the switching between state (S1) and (S2) translated by the inputs, I_2 and I_1, respectively.

(32, 33). The opening of the tweezers is accomplished by adding the cysteine (Cys) input that removes the Hg^{2+} by ligation (34). Fig. 2*B* depicts the cyclic opened/closed configuration operation of these tweezers. Similarly, programming the arm domains Ia and IIb of tweezers β to be pH sensitive stimulates the switchable opening/closing of this tweezers by H^+/OH^- inputs, Fig. 2*C*. At acidic pH the arms form the i-motif (35), thus releasing the linker unit, whereas at pH = 7.2, the i-motif is destroyed, resulting in the stabilization of the closed tweezers. The pH-switchable activities of tweezers β are demonstrated in Fig. 2*D*, using F_2 as the fluorescent label. Tweezers γ represent the trivial configuration, where the linker input (L) hybridized to the arms in the closed configuration is released from the structure by the complementary antilinker input (AL) that opens the tweezers (Fig. 2 *E* and *F*). The sequences of the nucleic acid components in tweezers α, β, and γ are presented in Table S1 and Fig. S1. It should be noted that the linker is common to all the three tweezers, and thus the closed configurations of tweezers α and β can be opened by the complementary hybridization of the antilinker strand to the linker. Thus, the simplest machines use any one of the pairs of tweezers presented in Fig. 2 *A*, *C*, or *E*. For each pair there are two possible inputs that either retain the state of the device or change its state. In Fig. 2*G* we show schematically the operation of a single tweezers, together with the corresponding input/output. In this simple automaton the configuration of the tweezers and the state of the machine are identical. This feature will change, however, when the number of tweezers is increased (*vide infra*).

Realizing that any of the tweezers can exist in two configurations, one may enhance the complexity of the device to reveal a richer number of configurations by the coupling of any of two tweezers (αβ, βγ, αγ). These pairs of tweezers may be instructed by the appropriate inputs (Fig. 3 *A*–*C*). To successfully operate each of the two-tweezers systems, the design of the tweezers must follow some energetic stabilization rules, where the sequences of domains Ia and IIb in the tweezers arms and the sequence of the linker play a very significant role (see Fig. 1*B*). In the αβ tweezers system, the tweezers are designed as follows: (*i*) The complementary region between each arm of tweezers β and the linker lacks T-T mismatches that are capable to form T-Hg^{2+}-T complexes in the presence of Hg^{2+}; (*ii*) the number of complementary bases between the linker and tweezers β should yield a duplex structure at neutral pH that exhibits lower stability as compared to the stability of the duplex structures generated between the linker and the arms of tweezers α, in the presence of Hg^{2+}. Fig. 3*A* shows the combination of tweezers α and β. While in the presence of Hg^{2+} tweezers α are closed due to the synergistic T-Hg^{2+}-T bridges and tweezers β are open; the elimination of the Hg^{2+} ions by cysteine energetically favors the hybridization of the linker to tweezers β. The readdition of Hg^{2+} ions regenerates the closed tweezers α and the open configuration of tweezers β. The concurrent operation of the two tweezers, αβ, is monitored by labeling tweezers α with fluorophore F_1 (λ_{em} = 600–650 nm) and the quencher (Q_1) and labeling tweezers β with fluorophore F_2 (λ_{em} = 700–750 nm) and the quencher (Q_2). Fig. 3*A*, panel II, depicts the cyclic activation of tweezers αβ by the repeated additions of Hg^{2+}/cysteine. To fullfil the energetic requirements discussed above, the sequence of the linker was optimized (see Table S2). Also, to allow the two-way operation of the β, γ tweezers system, we encode significant structural information into the base sequences of the different nucleic acids: (*i*) The number of complementary bases between the linker and tweezers γ should yield a duplex structure that has a lower stability compared to the duplex structures generated between the linker and each of the arms of tweezers β. This would preserve tweezers β in the closed configuration prior to the

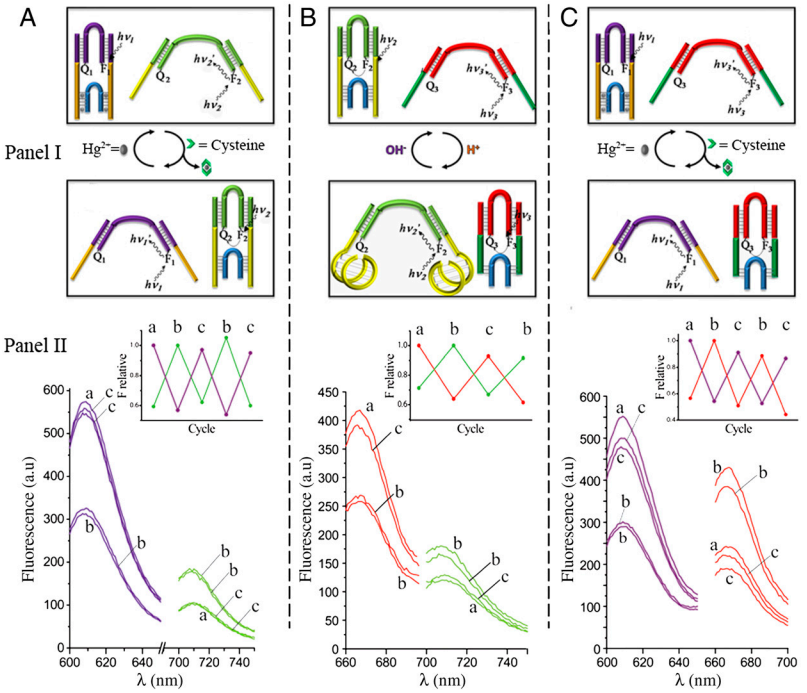

Fig. 3. (*A*) Concurrent activation of tweezers α and β using Hg^{2+} and cysteine as inputs that form the configuration (01) and (10), respectively (see panel I). Panel II: Fluorescence spectra corresponding to the configurations of the respective tweezers components. Tweezers α is followed at $\lambda = 600$–650 nm (purple). Tweezers β is monitored at $\lambda = 700$–750 nm (green): (a) Initial configuration of the tweezers, (10), with no added input. (b) After the addition of Hg^{2+} as input. (c) After the addition of the cysteine input. Inset: Cyclic activation of the two tweezers between configurations (01) (b) and (10) (c). (*B*) Concurrent activation of tweezers β and γ using H^+ and OH^- as inputs that form the configurations (10) and (01), respectively (see panel I). Panel II: Fluorescence spectra corresponding to the configurations of the respective tweezers components. Tweezers γ is followed at $\lambda = 660$–700 nm (red). Tweezers β is monitored at $\lambda = 700$–750 nm (green): (a) Initial configuration of the tweezers, (01), with no added input, at pH = 7.2. (b) After the addition of H^+ as input. (c) After the addition of the OH^- as input. Inset: Cyclic activation of the two tweezers between configurations (10) (b) and (01) (c). (*C*) Concurrent activation of tweezers α and γ using Hg^{2+} and cysteine as inputs that form the states (01) and (10), respectively (see panel I). Panel II: Fluorescence spectra corresponding to the configurations of the respective tweezers components. Tweezers α is followed at $\lambda = 600$–650 nm (purple). Tweezers γ is monitored at $\lambda = 660$–700 nm (red): (a) Initial configuration of the tweezers, (10), with no added input. (b) After the addition of Hg^{2+} as input. (c) After the addition of the cysteine input. Inset: Cyclic activation of the two tweezers between configurations (01) (b) and (10) (c).

folding of i-motif structure, while tweezers γ is in the open configuration. (*ii*) Sufficient base pairings between the linker and the arms of tweezers γ is needed in order to allow, at room temperature, the hybridization and closure of tweezers γ upon release of the linker from tweezers β at acidic pH. (*iii*) The number of complementary bases of the linker to the arms of tweezers β should be carefully controlled so that the linker can be released once the i-motif structure is formed. Fig. 3*B* shows the analogous activation of tweezers β and γ by pH inputs. While at basic pH tweezers β are in the closed structure, tweezers γ are in the open configuration. At acidic pH as input tweezers β open due to the formation of the i-motif structure, and tweezers γ close due to the hybridization with the linker released by tweezers β. At basic pH the i-motif structure is destroyed, and the original tweezers configurations are regenerated. By the labeling of tweezers γ with fluorophore F_3 ($\lambda_{em} = 660$–700 nm) the concurrent opening and closure of tweezers β,γ is demonstrated, as depicted in Fig. 3*B*, panel II. Similarly, the set of the concurrent operations of tweezers α,γ was accomplished as shown in Fig. 3*C*. While tweezers α exists in the T-Hg^{2+}-T-bridged closed configuration, addition of cysteine releases the linker that bridges tweezers γ into the closed configuration. By the readdition of Hg^{2+} ions, the original configurations of tweezers α,γ are regenerated. Fig. 3*C*, panel II, depicts the concurrent operation of tweezers α,γ by following the fluorescence features of F_1 and F_3 . Furthermore, control experiments indicated that the photophysical properties of the different fluorophores were not affected by the different inputs.

Realizing that a combination of each of the two tweezers can be cycled between closed and open configurations using the appropriate inputs, one may mix the three tweezers structures and one linker unit to form the four states (S5–S8) shown in Fig. 4*A* that are interconverted by the appropriate inputs. In each of these states two of the tweezers are open and one is in the closed structure to yield the configurations 011, 101, 110, and 011. For example, in configuration 011, S7, tweezers α are stabilized by the thymine- Hg^{2+}- thymine bridges in the closed structure and are transformed to the 101 configuration, S8, by interaction with cysteine resulting in the closure of tweezers β. The latter configuration translates at an acidic input into the configuration 110, S5, and upon reaction with Hg^{2+} ions as input the assembly 110 is converted to configuration 011, S6, resulting in the closure of tweezers α. One should note, however, that the 011 configuration in the state S5 and in the state S6 represent different states, because they exist in different pH environments. Thus, despite the similar optical transduction signals defining the configurations of the composited three tweezers, the unique definition of the state of the system requires the identification of the mode of formation (input) of the respective configuration. The inputs and respective outputs are indicated on the arrows representing the transitions between the different states. The fluorescence intensities providing the output that corresponds to each of the states are depicted in Fig. 4*B*, whereas the kinetics corresponding to the translation of the different state is shown in Fig. 4*C*.

The number of configurations (and states) of the tweezers automata may be further increased by introducing the linker and antilinker as inputs. Fig. 5 depicts schematically the set of eight possible configurations of the three tweezers systems and the set of 16 states of the automaton consisting of the three tweezers in the form of a central rhombus of the 111 configurations of the machine and four arms of the other states, where colored arrows

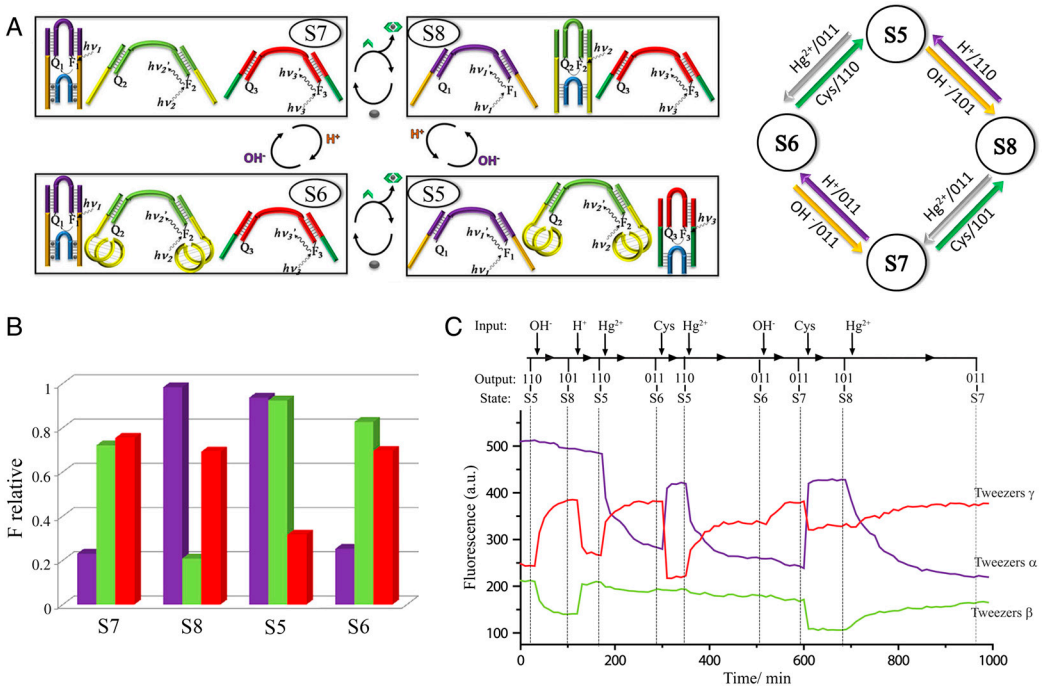

Fig. 4. (*A*) Schematic presentation of four possible states of a three-tweezers α,β,γ automata using one equivalent of the linker that can close any of the three tweezers. The respective configurations of the tweezers are monitored at $\lambda = 600$–650 nm, F_1 (for tweezers α), at $\lambda = 700$–750 nm, F_2 (for tweezers β) and at $\lambda = 660$–700 nm, F_3(for tweezers γ). (*B*) Fluorescence intensities corresponding to configurations of the four different states of the automaton depicted in *A*. Purple column corresponds to tweezers α, green column, tweezers β, and red column, tweezers γ (F relative is estimated according to the details given in Fig. S4.) (*C*) Time-dependent fluorescence intensities corresponding to the different configurations shown in *A* resulting from the transition between states induced by the different inputs. The initial state is S5 (configuration 110). The fluorescence intensities of the different tweezers are shown by different colors: purple, tweezers α; green, tweezers β; red, tweezers γ. Arrows on top indicate the time of application of the respective input.

indicate the input that translates each of the states to the corresponding other state. The central rhombus is surrounded by three additional coaxial generations of rhombi states. While the translation in each of the rhombi proceeds by the application of the Hg^{2+}/cysteine or H^+/OH^- inputs, the translation of a state from one rhombus to another requires the addition of linker(L)/antilinker(AL) inputs. The inputs and respective outputs are indicated on the arrows corresponding to the transitions between the states. The operation of the 16-states automaton is depicted in Fig. 6, where the translation of the states in each of the rhombi is followed by the fluorescence intensities of the respective configurations (Fig. 6 *A*–*C*). The translation of the state from one rhombus to another is shown in Fig. 6*D*, using the linker and antilinker as inputs. (The fluorescence spectra of all of the configurations and their cyclic operation are provided in Fig. S2.) The operation of the network of 16 states requires the appropriate design of the relative energetic of the closed/opened configurations in the presence of the respective inputs. (For the detailed energy relations see Fig. S3.) Furthermore, we note that the transitions across the three configurations of the tweezers can be cycled for at least six times, without notable perturbation of the system. We find that the least stable component in the system is ROX (F_1) that undergoes bleaching. Obviously, the open/closed configurations of the different tweezers are not complete. An open or closed tweezer is defined as a population of ≥60%. For the precise populations of the open/closed components in the different states, see Fig. S4.

The machine reported here is a finite-state automaton that we model as a "finite-state machine" (36, 37). Unlike a combinational gate, the output of a finite-state machine is determined not only by the input but also by the present state of the machine. We shall further discuss the machine with reference to the finite memory of its history (38, 39). To validate the proposed model we note that at any stage of operation a finite-state machine is characterized by an input, an output, and a state. The identification of the input and output is clear from the experiment and is shown in Fig. 1*A*. The input induces the transition to the next stage and is one of the six operations, e.g., add Hg^{2+}, identified in Fig. 1*A* and subsequent figures. The output is the fluorescence or, equivalently, the triplet of binary digits that specifies the configuration of the tweezers. To identify what specifies the state of the machine we go back to the formal characterization of a state: The state of a finite-state machine at a given stage together with the input at that stage specifies the output at that stage and specifies the state of the machine at the next stage. Schematically:

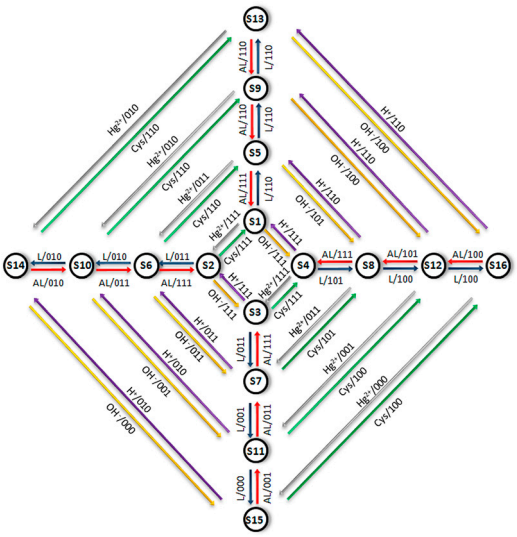

Fig. 5. Scheme of all 16 states of the three tweezers α, β, γ automaton. Color of arrows indicates the input translating one state to another (Hg^{2+}, gray; cysteine (Cys), green; H^+, purple; OH^-, orange; linker(L), blue; antilinker (AL), red. The inputs and respective outputs (input/output) are indicated on the arrows corresponding to the transitions between the states.

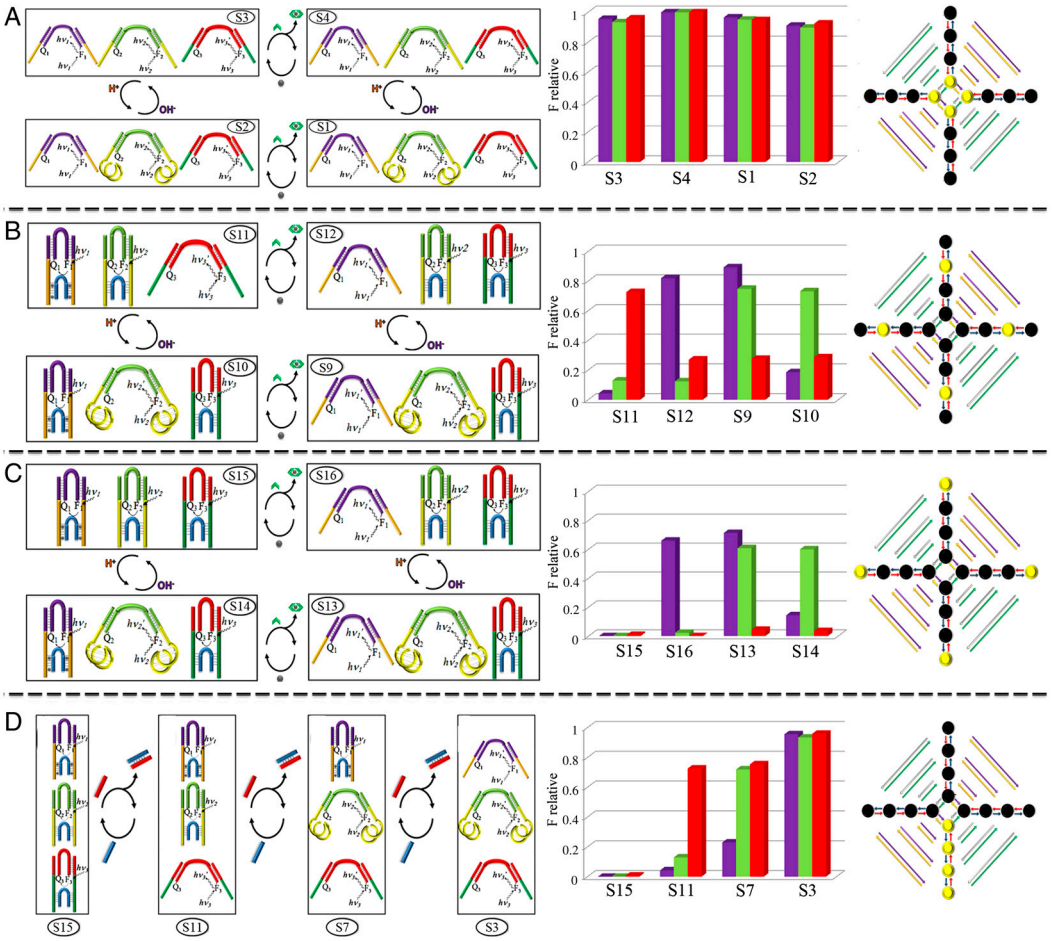

Fig. 6. Operation of the three-tweezers automaton using the different inputs, the respective fluorescence intensities of the different configurations, and the identification of the states in the schematic the coaxial rhombi diagram shown in Fig. 5. (*A*) Translation across all possible open three-tweezers states (inner rhombus marked yellow). (*B*) Translation across the four three-tweezers states shown in the third generation of rhombi states (yellow). (*C*) Translation across the four three-tweezers states in the fourth rhombi generation (yellow). (*D*) Translation across of the interrhombi states of the three tweezers, lower arm (yellow).

Current state and current input ⇒ present output

Current state and current input ⇒ next state

Toward defining the notion of a finite memory it is convenient to cast the characterization in words as a pair of equations for the present output and for the next state $z_\nu = f_z(x_\nu, s_\nu)$, $s_{\nu+1} = f_s(x_\nu, s_\nu)$. Here x_ν, z_ν and s_ν are, respectively, the input, output, and state at stage $\nu, \nu = ..,3,4,5..$ For our machine it is convenient to identify the variables that define the state after we first discuss the notion of a finite memory, as follows. Given the present state and the present input the transition table of the machine, Fig. S5, specifies the output. We are, however, interested to know if the machine remembers its past and, if so, how far back? What we can observe are outputs. What we can control are inputs. So the operational question is whether the output of the present stage can be predicted given the present stage input and a finite number of past inputs and outputs. If it can then the memory is said to be finite. The equation that defines the range μ of the finite memory expresses the output as $z_\nu = f(x_\nu, x_{\nu-1}, ... x_{\nu-\mu}, z_{\nu-1}, z_{\nu-2}, .., z_{\nu-\mu})$. The present output does not have to depend on all the variables shown, but going back only to a value of $\mu - 1$ is not sufficient. (For the mathematical expression of the next state of the machine see SI Appendix.) The mathematical result is that the present state is the history of the operation up to and including μ stages back. We now show that for our machine $\mu = 3$. For example, in Fig. 5, the right arm includes two 100 configurations that upon treatment with Hg^{2+} yields two configurations, 001 and 000, respectively, while the two configurations 110 (upper arm) are translated to the optically indistinguishable configurations 010 upon the addition of Hg^{2+} ions. Thus, the triplet of numbers of the configuration is insufficient to specify the state of the machine, and definition of the preceding steps generating the state is essential to identify a unique state of the machine. For example, the distinction between the 100 configurations (right arm) is obvious by following the fate of the distinct configurations 001 and 000 upon addition of cysteine, but the addition of OH^- to configurations 110 (upper arm) is insufficient to distinguish between the 100 configurations. Careful examination of Fig. 5 reveals that for the unique identification of apparently indistinguishable configurations the definition of up to three preceding steps is required. In other words, a state of our finite-state machine requires specifying the configuration of the tweezers and inputs for up to three preceding steps. It should be noted that any state can be generated from any other state depending on the applied inputs. The scheme of the 16 states of the instructive inputs and the respective outputs are show in Fig. 5. (For a detailed transition table, see Fig. S5.)

In conclusion, in the present study we adapted concepts of DNA machines (tweezers) to design an enzyme-free all-DNA automaton. The resulting finite-state machine reveals an interesting and potentially useful feature where the state of the system is not simply defined by the configurations of the molecules but by the "history" of formation of the configuration. While this property of acquired response is common in biosystems, we here introduce a man-made DNA composite mimicking this behavior. For a given sequence code of the linker/antilinker inputs, the sequence of states that are reached can be controlled by the sequence of inputs. We further show that by changing the sequence code of the linker/antilinker inputs, the relative energetic of the open/closed tweezers may be altered, thus leading to the programmability of the system. (For examples, see Fig. S6.) This opens the way to programmable machines. The use of pH or metal ions as inputs, and the controlled release or uptake of single stranded nucleic acids (antisense), might suggest the application of such automata in future nano-medical devices, where the

sensing of the appropriate biomarkers (inputs) is followed by the logic release of antisense units. A future potential application of such automata device could be to define the past exposure or nonexposure of a state to a certain input.

Material and Methods

Materials. MES acid hydrate, 2-(*N*-morpholino)ethanesulfonic (MES) acid potassium salt, sodium nitrate, and mercury (II) acetate were purchased from Sigma-Aldrich. L-cysteine hydrochloride was purchased from Fluka. Modified DNA oligonucleotides [(**1**), (**5**), and (**8**)] were purchased from Integrated DNA Technologies. All other oligonucleotide sequences were purchased from Sigma-Genosys. Ultrapure water from a NANOpure Diamond source was used in all of the experiments.

Instrumentation. Light emission measurements were performed using a Cary Eclipse Fluorimeter (Varian Inc.). The excitation of ROX, Cy5.5 and Cy5 were performed at 588, 680, and 648 nm, respectively. The emission of ROX, Cy5.5 and Cy5 were followed at $\lambda_{em} = 600$–650 nm, $\lambda_{em} = 700$–750 nm, and $\lambda_{em} = 660$–700 nm, respectively.

Assay. The system of tweezers α described in Fig. 2*A* included (**1**)–(**4**), 0.5 μM each, in an MES buffer solution (50 mM, 1 M $NaNO_3$). The solution was incubated at 90 °C for 5 min and cooled instantly to 25 °C for 40 min to hybridize the respective component. The cyclic operation of tweezers α was triggered by the addition of $Hg(COO)_2$, 5 μM or cysteine 10 μM, respectively.

The system of tweezers β described in Fig. 2*C* included the oligonucleotides (**4**)–(**7**), 0.5 μM each, in an MES buffer solution (50 mM, 1 M $NaNO_3$). The solution was incubated at 90 °C for 5 min and cooled instantly to 25 °C for 40 min to hybridize the components. The cyclic operation of the tweezers β was triggered by the addition of acetic acid (20%) or ammonia (10%) aqueous solutions to alter the pH of the solution to the values 5.2 and 7.2, respectively.

The system of tweezers γ described in Fig. 2*E* included the oligonucleotides (**4**) and (**8**)–(**11**), 0.5 μM each, in an MES buffer solution (50 mM, 1 M $NaNO_3$). The solution was incubated at 90 °C for 5 min and cooled instantly to 25 °C for 40 min to hybridize the components. The cyclic operation of the tweezers β system was activated by the addition of the nucleic acids (**4**) or (**11**), respectively.

The two-tweezers systems αβ, βγ, and αγ, described in Fig. 3 *A*–*C* consisted of the oligonucleotides (**1**)–(**7**), (**4**)–(**10**), and (**1**)–(**4**) (**8**)–(**10**), respectively, at a concentration of 0.5 μM for each oligonucleotide, in MES buffer solutions (50 mM, 1 M $NaNO_3$). The solutions were incubated at 90 °C for 5 min and cooled instantly to 25 °C for 40 min to allow the hybridization of the components. Tweezers α/β or α/γ systems were activated by the addition of $Hg(COO)_2$, 5 μM, or cysteine, 10 μM . The cyclic operation of tweezers β/γ system was activated by adding acetic acid (20%) or ammonia (10%) aqueous solutions to the system.

The three-tweezers systems, as described in Figs. 4 and 6 were studied in an MES buffer solution (50 mM, 1 M $NaNO_3$). The system consisted of oligonucleotides (**1**)–(**3**) and (**5**)–(**10**), 0.5 μM each. The solution was incubated at 90 °C for 5 min and cooled instantly to 25 °C for 40 min to allow the hybridization of the components. Ammonia (10%), acetic acid (20%), $Hg(COO)_2$ 5 μM, or cysteine 10 μM were added into the systems to inconvert the states in each of the rhombi. For the translation of states from rhombus to another rhombus, the linker (**4**), 0.5 μM, and antilinker (**11**), 0.5 μM were added.

ACKNOWLEDGMENTS. Parts of this research are supported by the European Community FP7 FET-proactive NanoICT project MOLOC (215750) and by the United States Naval Research Laboratory. F.R. is director of research at Fonds National de la Recherche Scientifique, Belgium. J.E. acknowledges a Converging Technologies Fellowship (Israel Science Foundation).

1. Benenson Y (2009) Biocomputers: From test tubes to live cells. *Mol Biosyst* 5:675–685.
2. Riehemann K, et al. (2009) Nanomedicine-challenge and perspectives. *Angew Chem Int Edit* 48:872–897.
3. Simmel FC (2007) Towards biomedical applications for nucleic acid nanodevices. *Nanomedicine-UK* 2:817–839.
4. Voelcker NH, Guckian KM, Saghatelian A, Ghadiri MR (2008) Sequence-addressable DNA logic. *Small* 4:427–431.
5. Stojanovic M, Stefanovic D (2003) A deoxyribozyme-based molecular automata. *Nat Biotechnol* 21:1069–1074.
6. Elbaz J, et al. (2010) DNA computing circuits using libraries of DNAzyme subunits. *Nat Nanotechnol* 5:417–422.
7. Penchovsky R, Breaker RR (2005) Computational design and experimental validation of oligonucleotide-sensing allosteric ribozymes. *Nat Biotechnol* 23:1424–1433.
8. Benenson Y, Paz-Elizur T, Adar R, Keinan E, Shapiro E (2001) Programmable and autonomous computing machine made of biomolecules. *Nature* 414:430–434.
9. Niazov T, Baron R, Lioubashevski O, Katz E, Willner I (2006) Concatenated logic gates using four coupled biocatalysts operating in series. *Proc Natl Acad Sci USA* 103:17160–17163.
10. Seelig G, Soloveichik D, Zhang DY, Winfree E (2006) Enzyme-free nucleic acid logic circuits. *Science* 314:1585–1589.
11. Benenson Y, Gil B, Ben-Dor U, Adar R, Shapiro E (2004) An autonomous molecular computer for logical control of gene expression. *Nature* 429:423–429.
12. Rinaudo K, et al. (2007) A universal RNAi-based logic evaluator that operates in mammalian cells. *Nat Biotechnol* 25:795–801.
13. Win MN, Smolke CD (2008) Higher-order cellular information processing with synthetic RNA devices. *Science* 322:456–460.
14. Seeman NC (2005) From genes to machines: DNA nanomechanical devices. *Trends Biochem Sci* 30:119–125.
15. Beissenhirtz MK, Willner I (2006) DNA-based machines. *Org Biomol Chem* 4:3392–3401.
16. Liedl T, Sobey TL, Simmel FC (2007) DNA-based nanodevices. *Nano Today* 2:36–41.
17. Bath J, Turberfield AJ (2007) DNA nanomachines. *Nat Nanotechnol* 2:275–284.
18. Omabegho T, Sha R, Seeman NC (2009) A bipedal DNA brownian motor with coordinated legs. *Science* 324:67–71.
19. Shin JS, Pierce NA (2004) A synthetic DNA walker for molecular transport. *J Am Chem Soc* 126:10834–10835.
20. Green SJ, Bath J, Turberfield AJ (2008) Coordinated chemomechanical cycles: A mechanism for autonomous molecular motion. *Phys Rev Lett* 101:139901.
21. Yin P, Choi HMT, Calvert CR, Pierce NA (2008) Programming biomolecular self-assembly pathways. *Nature* 451:318–322.
22. Elbaz J, Tel-Vered R, Freeman R, Yildiz HB, Willner I (2009) Switchable motion of DNA on solid supports. *Angew Chem Int Edit* 48:133–137.
23. Chhabra R, Sharma J, Liu Y, Yan H (2006) Addressable molecular tweezers for DNA-templated coupling reactions. *Nano Lett* 6:978–983.
24. Yurke B, Turberfield AJ, Mills AP, Jr, Simmel FC, Neumann JL (2000) A DNA-fuelled molecular machine made of DNA. *Nature* 406:605–608.
25. Elbaz J, Moshe M, Willner I (2009) Coherent activation of DNA tweezers: A "SET-RESET" logic system. *Angew Chem Int Edit* 48:3834–3837.
26. Elbaz J, Wang ZG, Orbach R, Willner I (2009) pH-Stimulated concurrent mechanical activation of two DNA "tweezers". A "SET-RESET" logic gate system. *Nano Lett* 9:4510–4514.
27. Tian Y, Mao C (2004) Molecular gears: A pair of DNA circles continuously rolls against each other. *J Am Chem Soc* 126:11410–11411.
28. Shlyahovsky B, et al. (2007) Proteins modified with DNAzymes or aptamers act as biosensors or biosensor labels. *J Am Chem Soc* 129:3814–3815.
29. Liu D, Balasubramanian S (2003) A proton-fuelled DNA nanomachine. *Angew Chem Int Edit* 42–5734–5736.
30. Modi S, et al. (2009) A DNA nanomachine that maps spatial and temporal pH changes inside living cells. *Nat Nanotechnol* 4:325–330.
31. Reif JR, Sahu1 S (2009) Autonomous programmable DNA nanorobotic devices using DNAzymes. *Theor Comput Sci* 410:1428–1439.
32. Clever GH, Kaul C, Carell T (2007) DNA-metal base pairs. *Angew Chem Int Edit* 46:6226–6236.
33. Miyake Y, et al. (2006) Mercury^{II}-mediated formation of thymine-Hg^{II}-thymine base pairs in DNA duplexes. *J Am Chem Soc* 128:2172–2173.
34. Lee JS, Ulmann PA, Han MS, Mirkin CA (2008) A DNA-gold nanoparticle-based colorimetric competition assay for the detection of cysteine. *Nano Lett* 8:529–533.
35. Gehring K, Leroy JL, Gueron M (1993) A tetrameric DNA structure with protonated cytosine-cytosine base pairs. *Nature* 363:561–565.
36. Gill A (1962) *Introduction to the Theory of Finite-State Machines* (McGraw-Hill, New York).
37. Kohavi Z (1978) *Switching and Finite Automata Theory* (McGraw-Hill, New York).
38. Simon JM (1959) A note on the memory aspects of sequence transducers. *IRE Trans on Circuit Theory* CT-6:26–29.
39. Gill A (1966) *Linear Sequential Circuits* (McGraw-Hill, New York).